

# Monitoring statistics of the ERS-2 scatterometer for ESA

## Cycle 162

(Project Ref. 22025/08/I-EC)

Hans Hersbach  
European Centre for Medium-Range Weather Forecasts,  
Shinfield Park, Reading, RG2 9AX, England  
Tel: (+44 118) 9499476, e-mail: dal@ecmwf.int

November 25, 2010

## 1 Introduction

The quality of the UWI product was monitored at ECMWF for Cycle 162. Results were compared to those obtained from the previous Cycle, as well for data received during the nominal period in 2000 (up to Cycle 59). No corrections for duplicate observations from overlapping ground stations were applied.

During Cycle 162 data was received between 21:04 UTC 18 October 2010 and 19:35 UTC 22 November 2010. Data was grouped into 6-hourly batches (centred around 00, 06, 12 and 18 UTC), and for all such batches, data was received.

Data is being recorded whenever within the visibility range of a ground station. For Cycle 162, data coverage was over the North-Atlantic, the Mediterranean, part of the Gulf of Mexico, an area in the Pacific west from the US, Canada and Central America (much improved compared to Cycle 161), and the area in between Antarctica and Australia (see Figure 2).

Time series of the asymmetry between the fore and aft incidence angles shows a stable behaviour.

Compared to Cycle 161, the UWI wind speed relative to ECMWF first-guess (FG) fields showed a slightly larger standard deviation (1.50 m/s, was 1.47 m/s). Bias levels were a bit less negative (on average -0.89 m/s, was -0.93 m/s).

Between 9 and 12 November 2010 the performance of UWI wind direction was found to be very poor, indicating a temporary problem at the ESACA de-aliasing. For at ECMWF de-aliased CMOD5-based winds, no deterioration was observed for that period.

Ocean calibration shows that inter-node and inter-beam dependencies of bias levels have reduced. Average bias levels were less negative (-0.54 dB, was -0.66 dB; see Figure 4).

The ECMWF operational assimilation and forecast system was updated on 9 November 2010. Among other things, an adjustment was made to diffusion in stable boundary layers near the surface, and scatterometer winds now take account for variation in stability in the surface layer (by assimilation as equivalent neutral wind). Although this latter change affects surface wind directly, only a modest impact is anticipated on the quality of model surface wind.

The Cycle-averaged evolution of performance relative to ECMWF first-guess (FG) winds is displayed in Figure 1. Figure 2 shows global maps of the over Cycle 162 averaged UWI data coverage and wind climate, Figure 3 for performance relative to FG winds.

## 2 ERS-2 statistics from 18 October 2010 to 22 November 2010

### 2.1 Sigma0 bias levels

The average sigma0 bias levels (compared to simulated sigma0's based on ECMWF model FG winds) stratified with respect to antenna beam, ascending or descending track and as function of incidence angle (i.e. across-node number) is displayed in Figure 4.

Compared to Cycle 161, inter-node and inter-beam dependencies between the fore and aft beam have slightly reduced. Average bias level was less negative (-0.54 dB, was -0.66 dB), being 0.15 dB more negative than for nominal data in 2000 (around -0.4 dB; see Figure 1 of the reports for Cycle 48 to 59). The asymmetry is somewhat worse than that of one year ago (see report for Cycle 152).

Long-term variations correlate with the yearly cycle, which, given the non-global coverage, is understandable. Therefore, the method of ocean calibration will probably only provide accurate information on calibration levels for globally or yearly averaged data sets.

The data volume of descending tracks was about 19% lower than for ascending tracks.

### 2.2 Incidence angles

From simple geometrical arguments it follows that variations in yaw attitude will lead to asymmetries between the incidence angles of the fore and aft beam. Indeed, this has been observed. Figure 5 gives a time evolution of this asymmetry. Also in this Figure, the occasions for which the combined  $k_p$ -yaw quality flag was set are indicated by red stars. The relation with incidence-angle asymmetries is obvious.

The behaviour was rather calm during Cycle 162.

After a prolonged minimum, solar activity is on the rise. A few large solar spots developed mid October 2010. The Earth was under the influence of solar storms around 24 October 2010, from 2 to 4 November 2010 and from 12 to 14 November 2010 (source:

www.spaceweather.com). These events did not seem to have an effect on ERS-2 attitude control.

### 2.3 Distance to cone history

The distance to the cone history is shown in Figure 6. Curves are based on data that passed all QC, including the test on the  $k_p$ -yaw flag, and subject to the land and sea-ice check at ECMWF (see cyclic report 88 for details).

Like for previous Cycles, time series are (due to lack of statistics) very noisy, especially for the near-range nodes. Most spikes were found to be the result of low data volumes.

Compared to Cycle 161, the average level was stable (1.22, was 1.23), and is higher (by 12%) than for nominal data (see top panel Figure 1).

The fraction of data that did not pass QC is displayed in Figure 6 as well (dashed curves).

### 2.4 UWI minus First-Guess wind history

In Figure 7, the UWI minus ECMWF first-guess wind-speed history is plotted. The history plot shows a few peaks, which are usually the result of low data volume.

Figure 11 displays the locations for which UWI winds were more than 8 m/s weaker (top panel), respectively more than 8 m/s stronger (lower panel) than FG winds. Like for Cycle 161, such collocations are isolated, and often indicate meteorologically active regions, for which UWI data and ECMWF model field show reasonably small differences in phase and/or intensity. Deviations near the poles are the result of imperfect sea-ice flagging.

Two examples for which UWI and ECMWF winds differ significantly are presented in Figure 12.

Average bias levels and standard deviations of UWI winds relative to FG winds are displayed in Table 1. From this it follows that the bias of UWI winds was slightly less negative (-0.89 m/s, was -0.93 m/s), being around the level of nominal data in 2000.

On a longer time scale seasonal bias trends are observed (see Figure 1). As was highlighted in previous cyclic reports, it is believed that the yearly trend is partly induced by changing local geophysical conditions.

The standard deviation of UWI wind speed versus ECMWF FG has, compared to Cycle 161, was slightly enhanced (1.50 m/s, was 1.47 m/s).

For Cycle 162 the (UWI - FG) direction standard deviations were mostly ranging between 20 and 40 degrees (Figure 8). However, between 9 and 12 November 2010 STDV was higher than 60 degrees, which indicates a temporary problem with the ESACA de-aliasing. As a result of this short period, average STDV for UWI wind direction was higher than usual, but lower than for Cycle 161 (31.8 degrees, was 36.8 degrees), which encountered similar problems. For at ECMWF de-aliased winds (Figure 10) performance is more stable (STDV 19.8, was 19.3 degrees).

	Cycle 161		Cycle 162	
	UWI	CMOD4	UWI	CMOD4
speed STDV	1.47	1.46	1.50	1.49
node 1-2	1.54	1.52	1.57	1.54
node 3-4	1.47	1.46	1.47	1.46
node 5-7	1.38	1.38	1.41	1.40
node 8-10	1.40	1.39	1.43	1.44
node 11-14	1.46	1.45	1.49	1.48
node 15-19	1.46	1.46	1.48	1.48
speed BIAS	-0.93	-0.93	-0.89	-0.88
node 1-2	-1.47	-1.45	-1.52	-1.49
node 3-4	-1.24	-1.20	-1.22	-1.16
node 5-7	-0.99	-0.96	-0.93	-0.89
node 8-10	-0.79	-0.79	-0.72	-0.71
node 11-14	-0.74	-0.75	-0.65	-0.67
node 15-19	-0.72	-0.74	-0.66	-0.68
direction STDV	36.8	19.3	31.6	19.8
direction BIAS	-1.9	-2.5	-2.7	-2.7

Table 1: Biases and standard deviation of ERS-2 versus ECMWF FG winds in m/s for speed and degrees for direction.

## 2.5 Scatterplots

Scatterplots of FG winds versus ERS-2 winds are displayed in Figures 13 to 16. Values of standard deviations and biases are slightly different from those displayed in Table 1. Reason for this is that, for plotting purposes, the in 0.5 m/s resolution ERS-2 winds have been slightly perturbed (increases scatter with 0.02 m/s), and that zero wind-speed ERS-2 winds have been excluded (decreases scatter by about 0.05 m/s).

The scatterplot of UWI wind speed versus FG (Figure 13) is very similar to that for (at ECMWF inverted) de-aliased CMOD4 winds (Figure 15). It confirms that the ESACA inversion scheme is working properly.

Winds derived on the basis of CMOD5 are displayed in Figure 16. The relative standard deviation is lower than for CMOD4 winds (1.46 m/s versus 1.52 m/s). Compared to ECMWF FG, CMOD5 winds are 0.35 m/s slower.

## Figure Captions

**Figure 1:** Evolution of the performance of the ERS-2 scatterometer averaged over 5-weekly Cycles from 12 December 2001 (Cycle 69) to 22 November 2010 (end Cycle 162) for the UWI product (solid, star) and de-aliased winds based on CMOD4 (dashed, diamond). Results are based on data that passed the UWI QC flags. For Cycle 85 two values are plotted; the first value for a global set, the second one for a regional set (for

details see the corresponding cyclic report). Dotted lines represent values for Cycle 59 (5 December 2000 to 17 January 2001), i.e. the last stable Cycle of the nominal period. From top to bottom panel are shown the normalized distance to the cone (CMOD4 only) the standard deviation of the wind speed compared to FG winds, the corresponding bias (for UWI winds the extremes in node-wise averages are shown as well), and the standard deviation of wind direction compared to FG.

**Figure 2:** Average number of observations per 12H and per 125km grid box (top panel) and wind climate (lower panel) for UWI winds that passed the UWI flags QC and a check on the collocated ECMWF land and sea-ice mask.

**Figure 3:** The same as Figure 2, but now for the relative bias (top panel) and standard deviation (lower panel) with ECMWF first-guess winds.

**Figure 4:** Ratio of  $\langle \sigma_0^{0.625} \rangle / \langle \text{CMOD4}(\text{FirstGuess})^{0.625} \rangle$  converted in dB for the fore beam (solid line), mid beam (dashed line) and aft beam (dotted line), as a function of incidence angle for descending and ascending tracks. The thin lines indicate the error bars on the estimated mean. First-guess winds are based on the in time closest (+3h, +6h, +9h, or +12h) T799 forecast field, and are bilinearly interpolated in space.

**Figure 5:** Time series of the difference in incidence angle between the fore and aft beam. Red stars indicate the occurrences for which the combined  $k_p$ -yaw flag was set.

**Figure 6:** Mean normalized distance to the cone computed every 6 hours for nodes 1-2, 3-4, 5-7, 8-10, 11-14 and 15-19). The dotted curve shows the number of incoming triplets in logarithmic scale (1 corresponds to 60,000 triplets) and the dashed one indicates the fraction of complete (based on the land and sea-ice mask at ECMWF) sea-located triplets rejected by ESA flags, or by the wind inversion algorithm (0: all data kept, 1: no data kept).

**Figure 7:** Mean (solid line) and standard deviation (dashed line) of the wind speed difference UWI - first guess for the data retained by the quality control.

**Figure 8:** Same as Fig. 7, but for the wind direction difference. Statistics are computed for winds stronger than 4 m/s.

**Figures 9 and 10:** Same as Fig. 7 and 8 respectively, but for the de-aliased CMOD4 data.

**Figure 11:** Locations of data during Cycle 162 for which UWI winds are more than 8 m/s weaker (top panel) respectively stronger (lower panel) than FG, and on which QC on UWI flags and the ECMWF land/sea-ice mask was applied.

**Figure 12:** A case in the North Atlantic on 2 November 2010 (top panel) and the Mediterranean for 8 November 2010 (lower panel). Red and blue barbs represent UWI winds and ECMWF FG winds, respectively.

**Figure 13:** Two-dimensional histogram of first guess and UWI wind speeds, for the data kept by the UWI flags, and QC based on the ECMWF land and sea-ice mask. Circles denote the mean values in the y-direction, and squares those in the x-direction.

**Figure 14:** Same as Fig. 13, but for wind direction. Only winds stronger than 4m/s are taken into account.

**Figure 15:** Same as Fig. 13, but for de-aliased CMOD4 winds.

**Figure 16:** Same as Fig. 13, but for de-aliased CMOD5 winds.

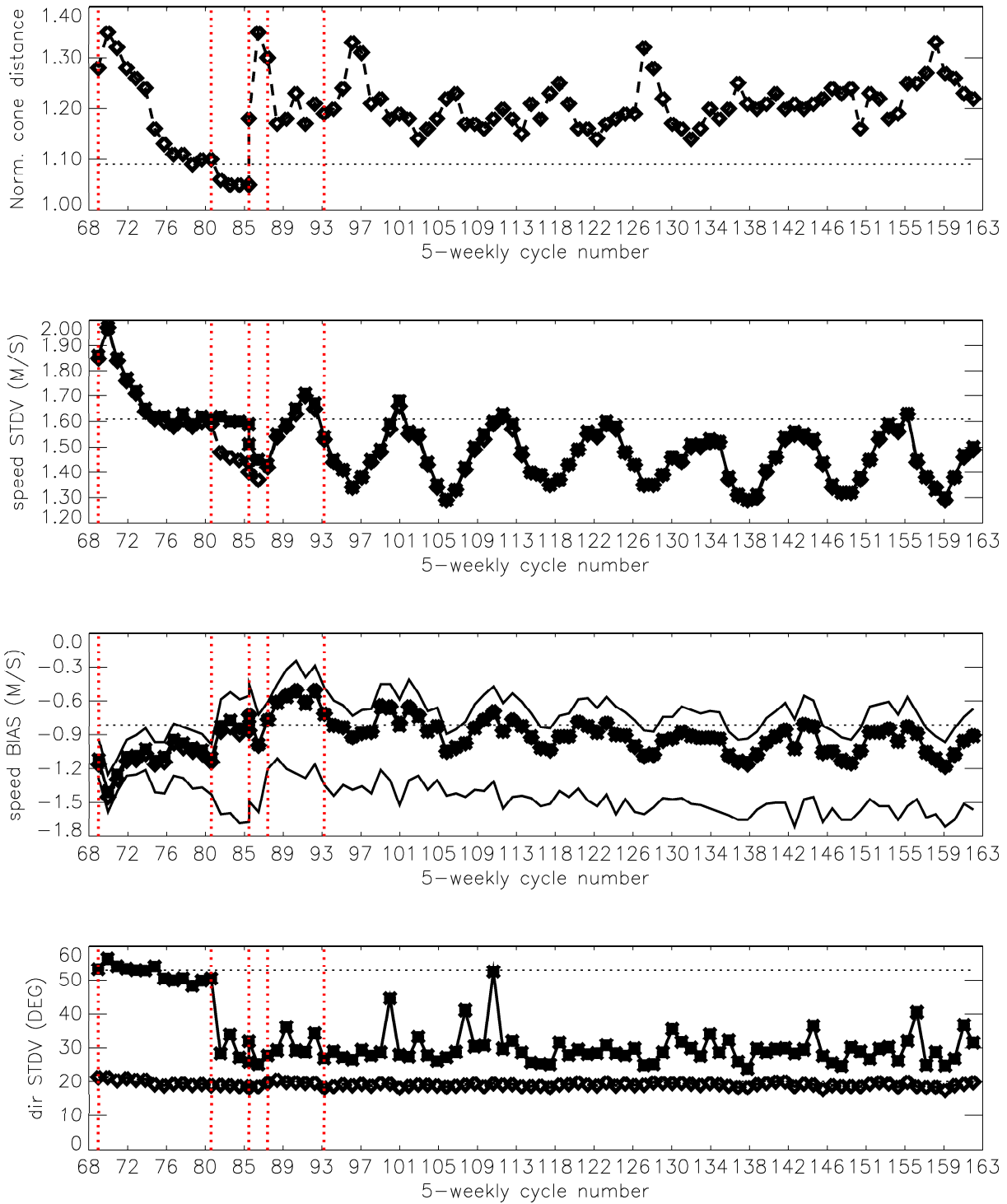
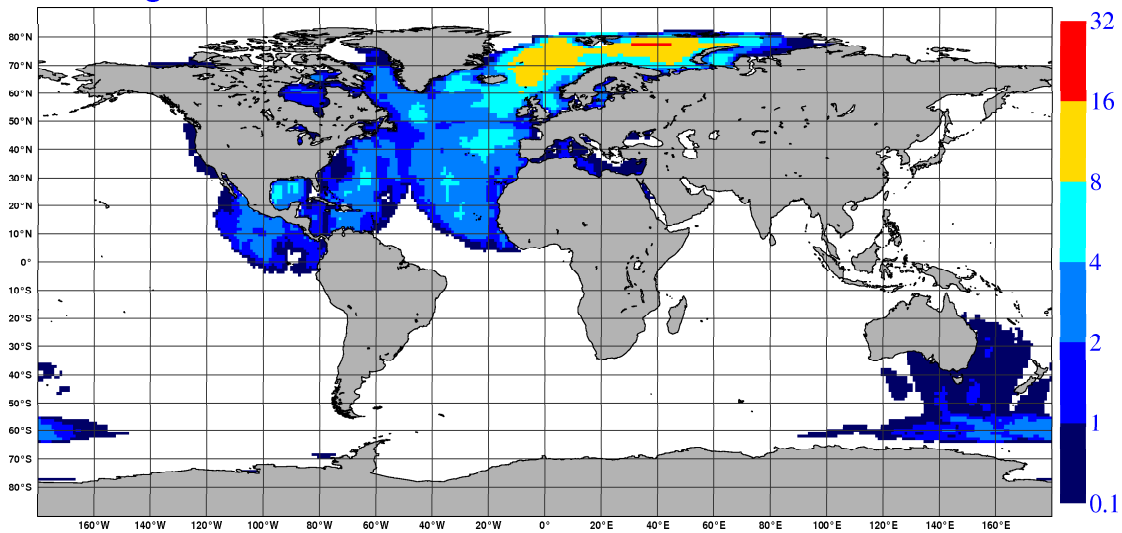


Figure 1

NOBS ( ERS-2 UWI ), per 12H, per 125km box  
average from 2010101900 to 2010112218 GLOB:2.11



AVERAGE ( ERS-2 UWI ), in m/s.  
average from 2010101900 to 2010112218 GLOB:6.72

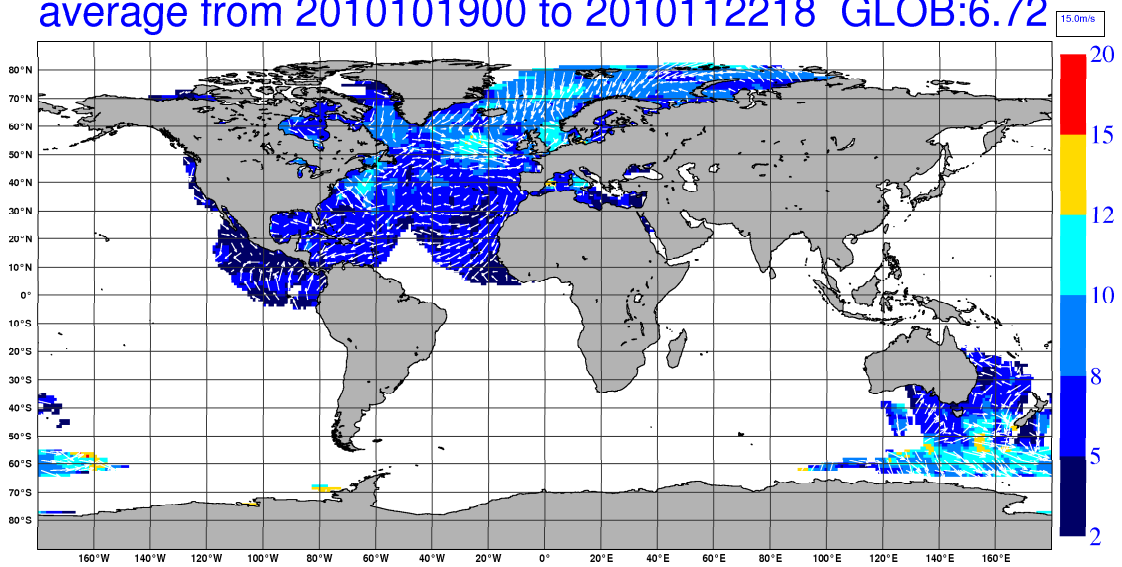
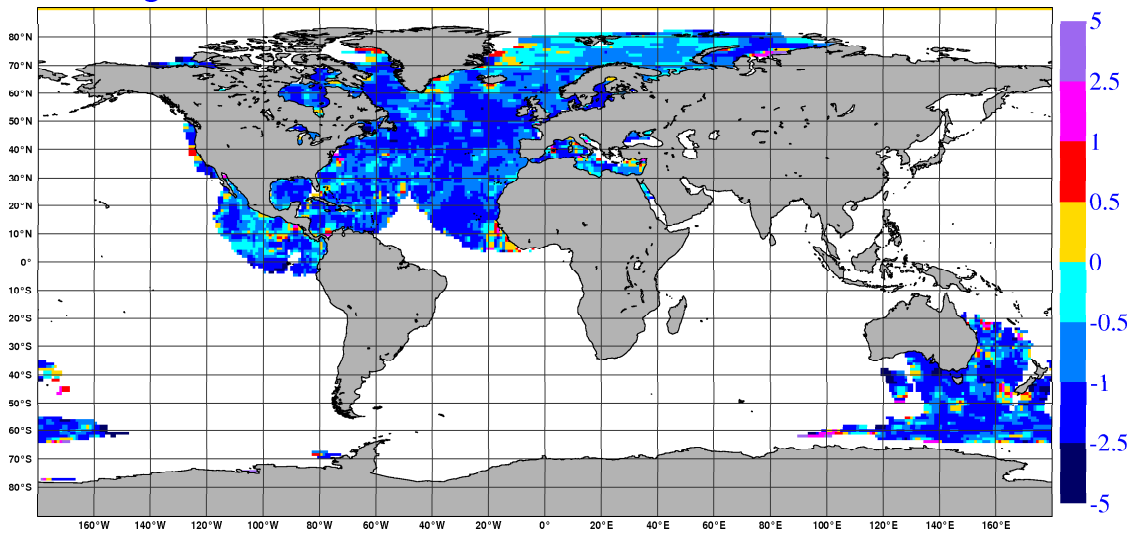


Figure 2

BIAS ( ERS-2 UWI vs FIRST-GUESS ), in m/s.  
average from 2010101900 to 2010112218 GLOB:-0.94



STDV ( ERS-2 UWI vs FIRST-GUESS ), in m/s.  
average from 2010101900 to 2010112218 GLOB:1.2

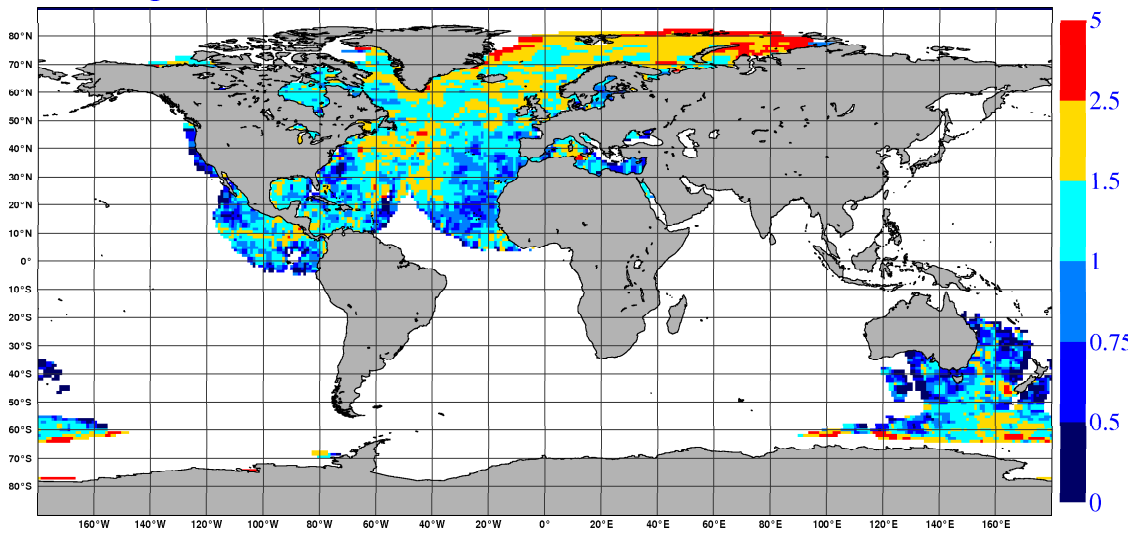


Figure 3



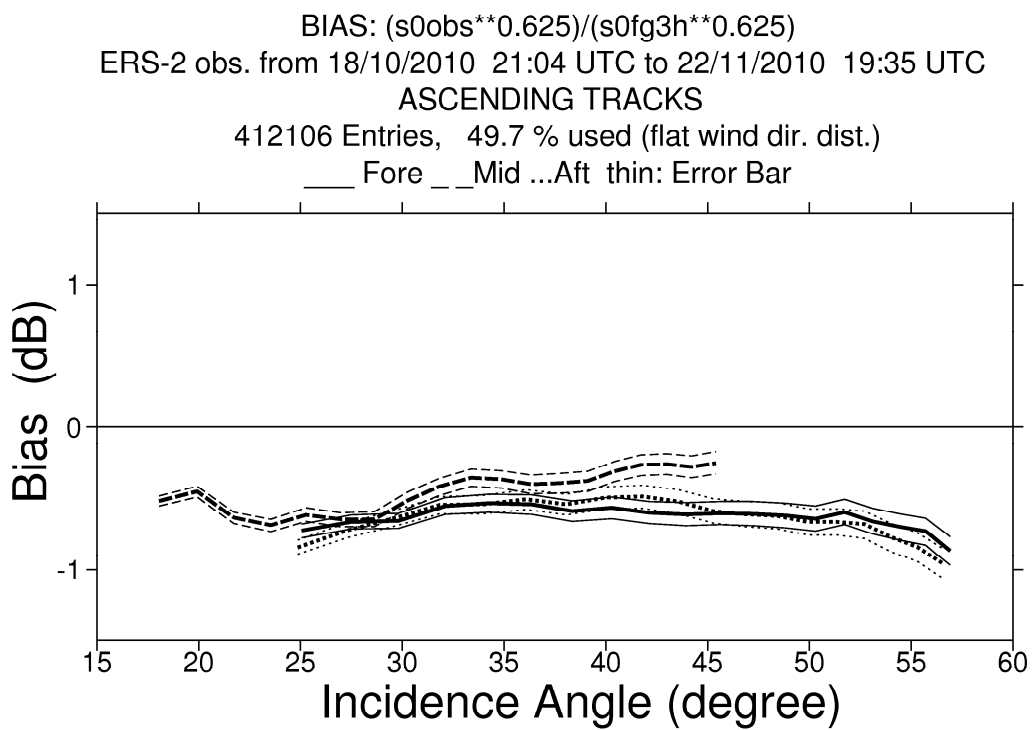
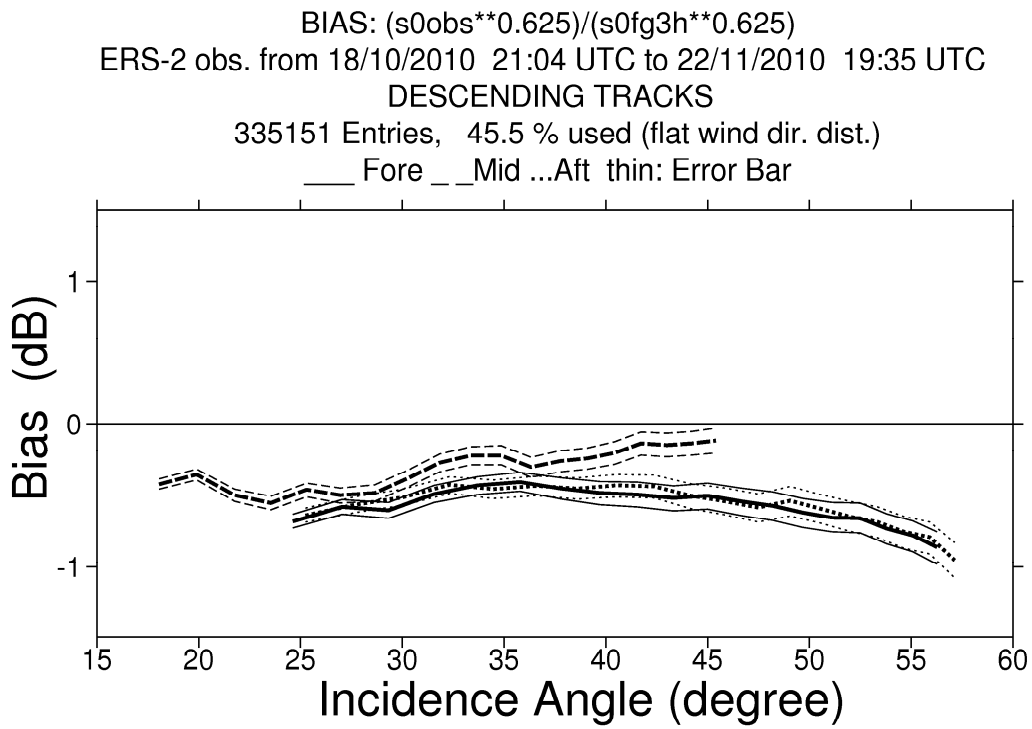


Figure 4

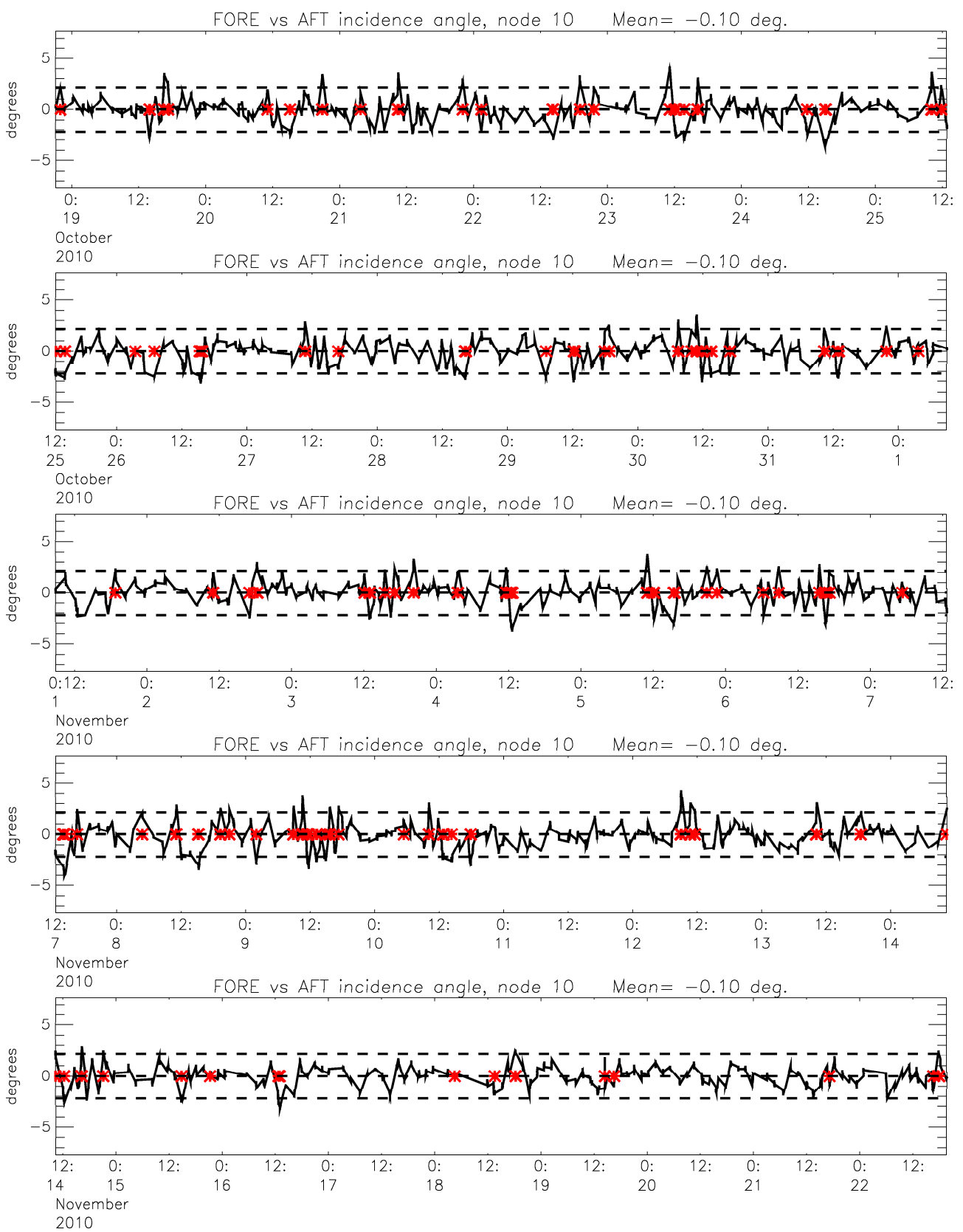


Figure 5

# Monitoring of Sigma0 triplets versus CMOD4 for ERS-2

from 2010101900 to 2010112218

(solid) mean normalised distance to the cone over 6 h

(dashed) fraction of complete sea-point observations rejected by ESA flag or CMOD4 inversion

(dotted) total number of data in log. scale (1 for 60000)

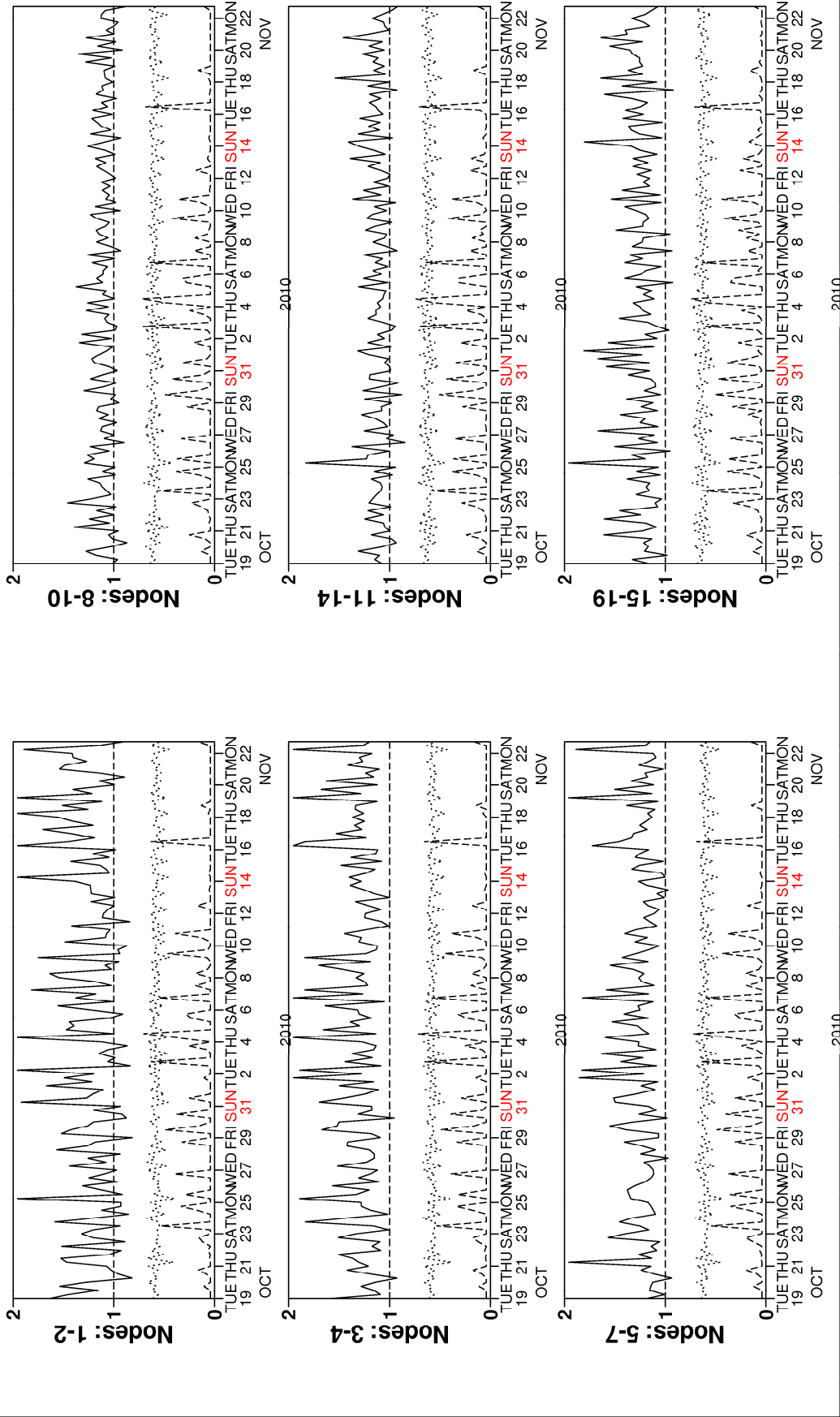


Figure 6

# Monitoring of UWI winds versus First Guess for ERS-2

from 2010101900 to 2010112218

(solid) wind speed bias UWI - First Guess over 6h (deg.)

(dashed) wind speed standard deviation UWI - First Guess over 6h (deg.)

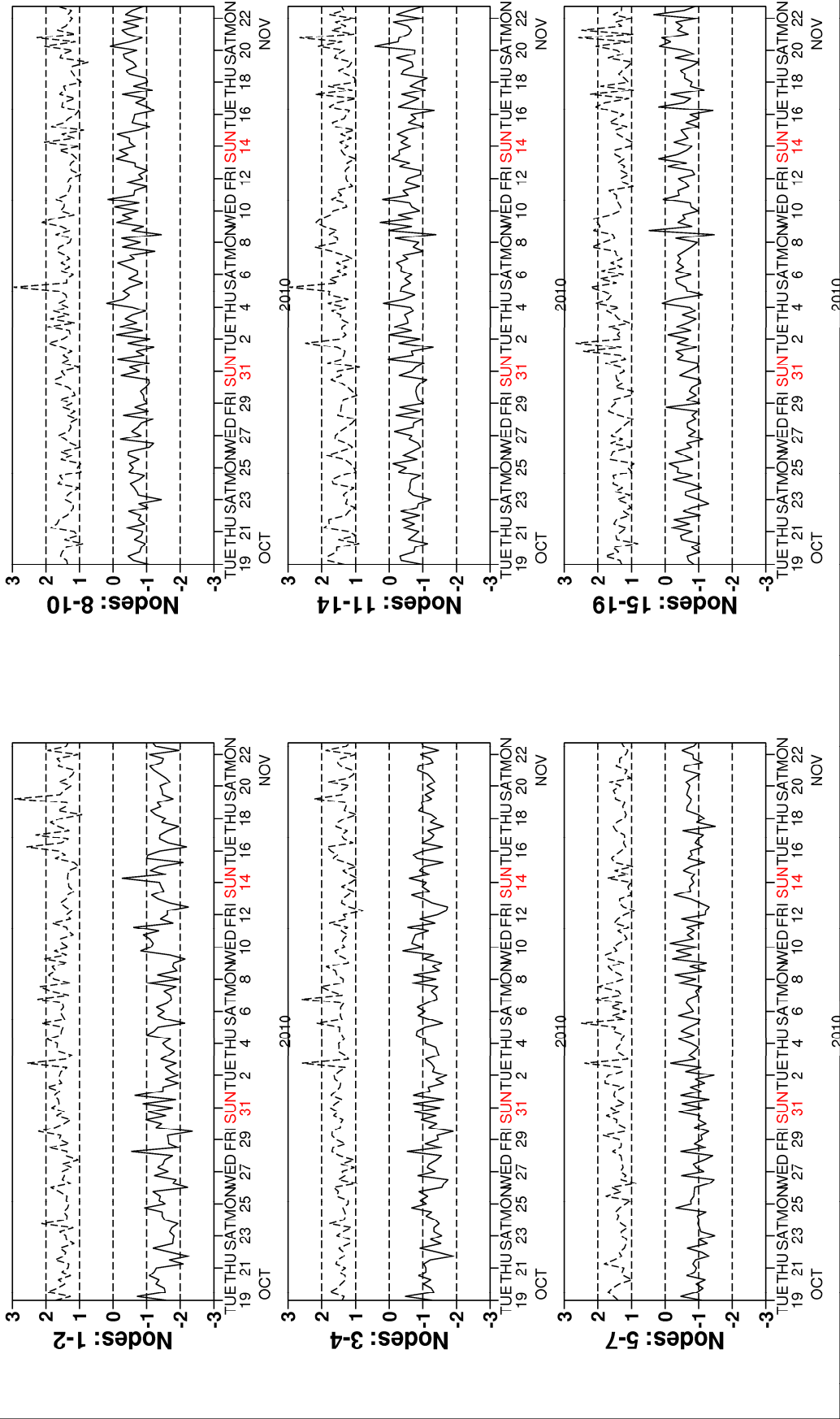


Figure 7

# Monitoring of UWI winds versus First Guess for ERS-2

from 2010101900 to 2010112218

(solid) wind direction bias UWI - First Guess over 6h (deg.)

(dashed) wind direction standard deviation UWI - First Guess over 6h (deg.)

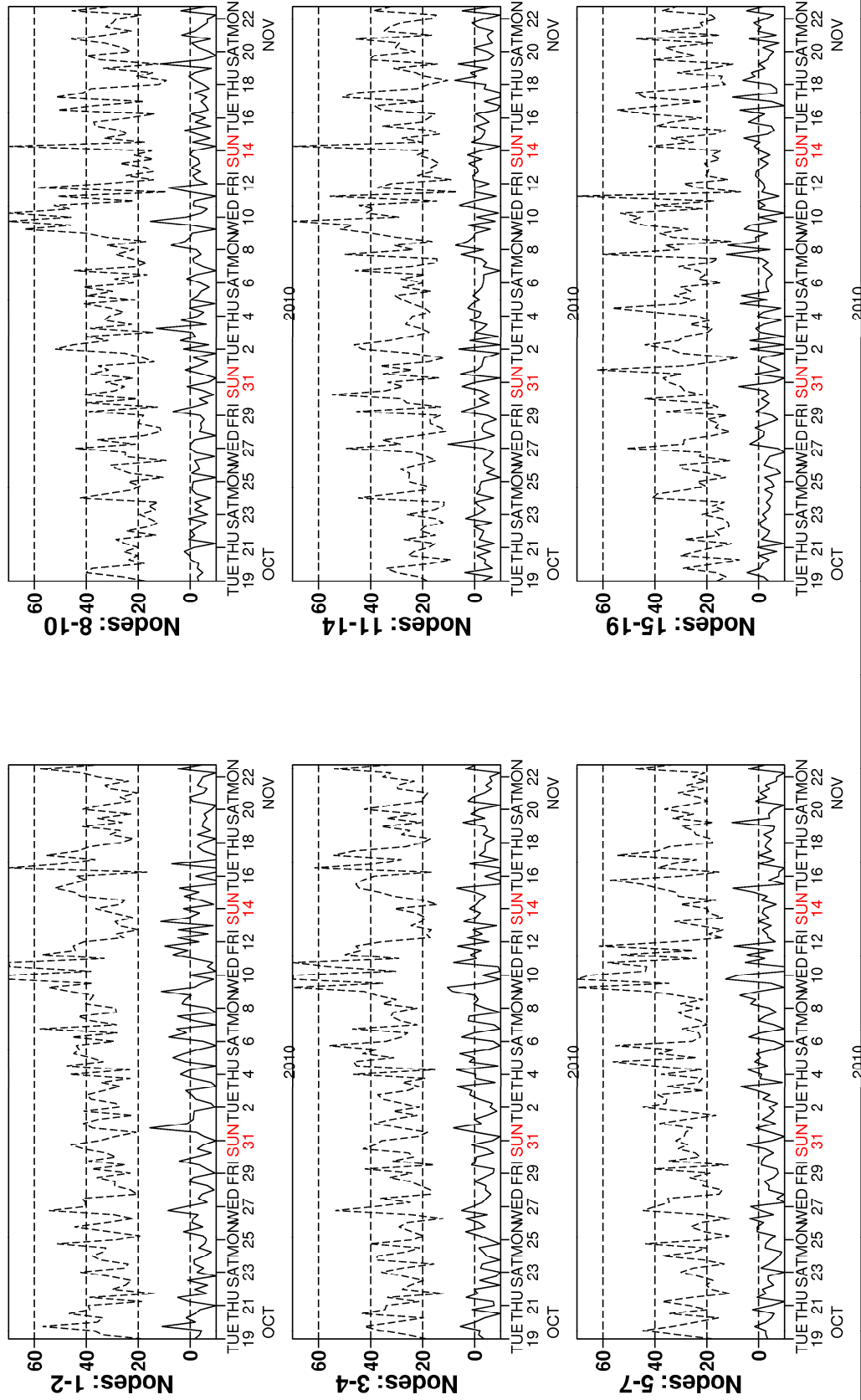


Figure 8

# Monitoring of de-aliased CMOD4 winds versus First Guess for ERS-2

from 2010101900 to 2010112218

(solid) wind speed bias CMOD4 - First Guess over 6h (deg.)

(dashed) wind speed standard deviation CMOD4 - First Guess over 6h (deg.)

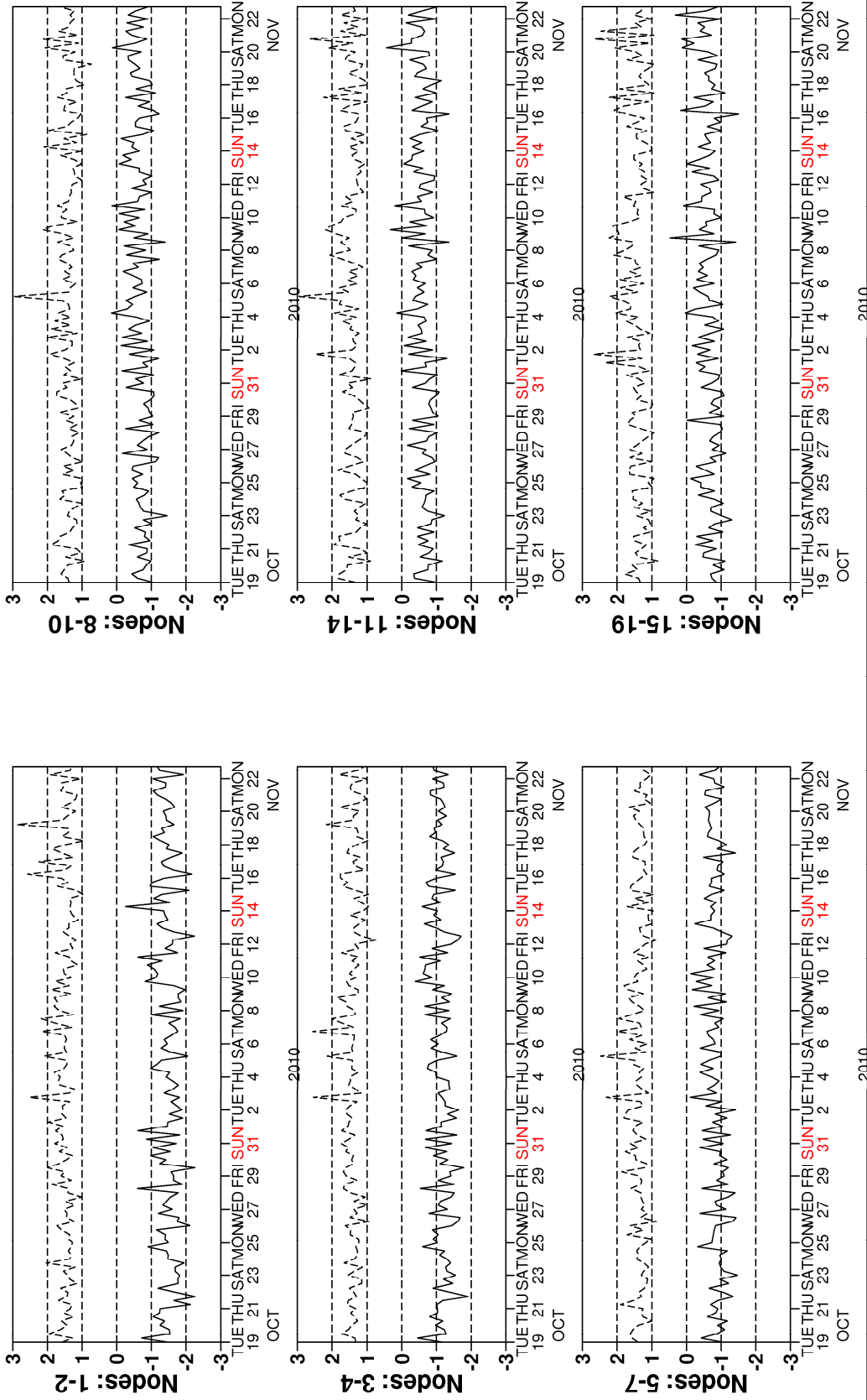


Figure 9

# Monitoring of de-aliased CMOD4 winds versus First Guess for ERS-2

from 2010101900 to 2010112218

(solid) wind direction bias CMOD4 - First Guess over 6h (deg.)

(dashed) wind direction standard deviation CMOD4 - First Guess over 6h (deg.)

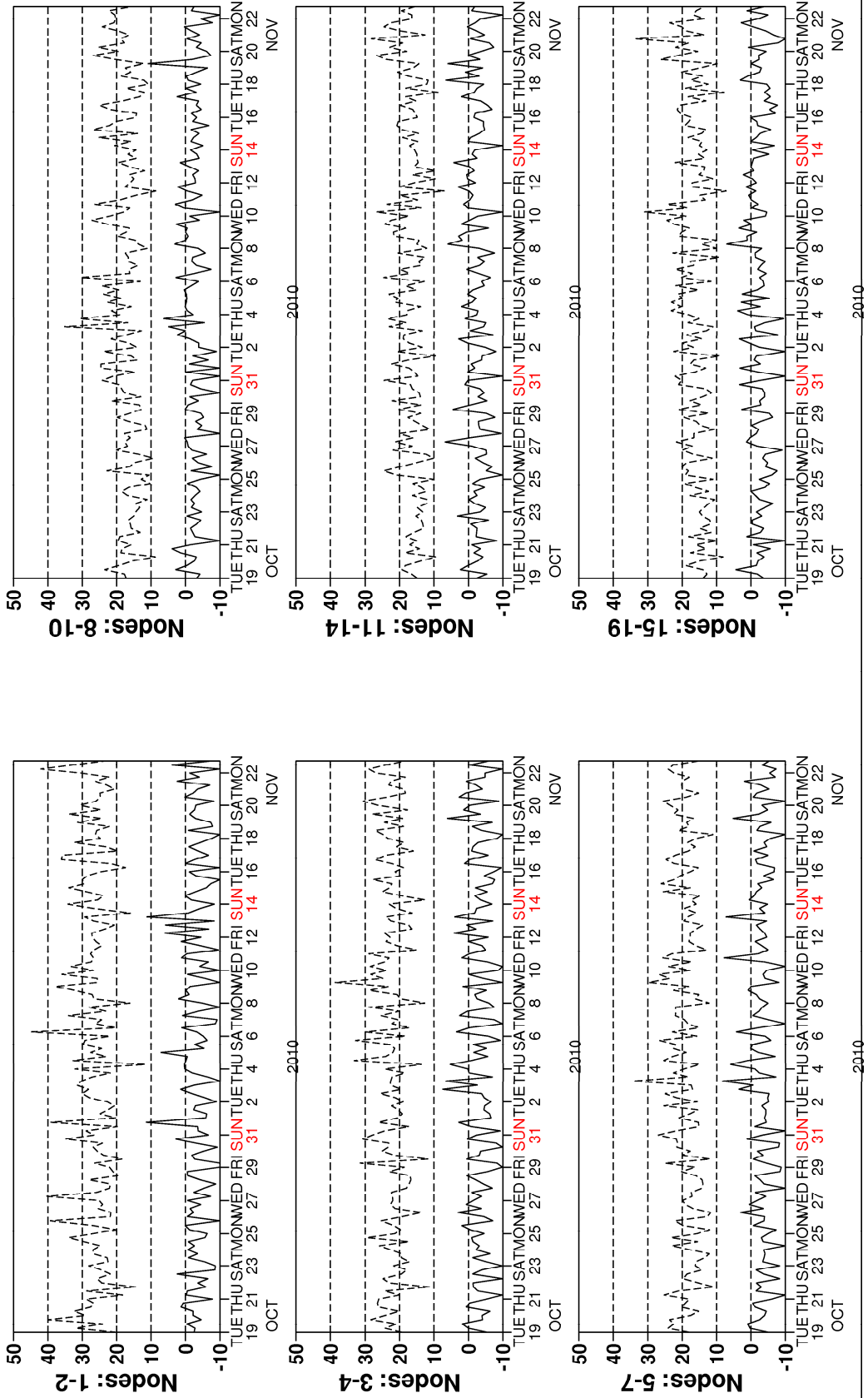
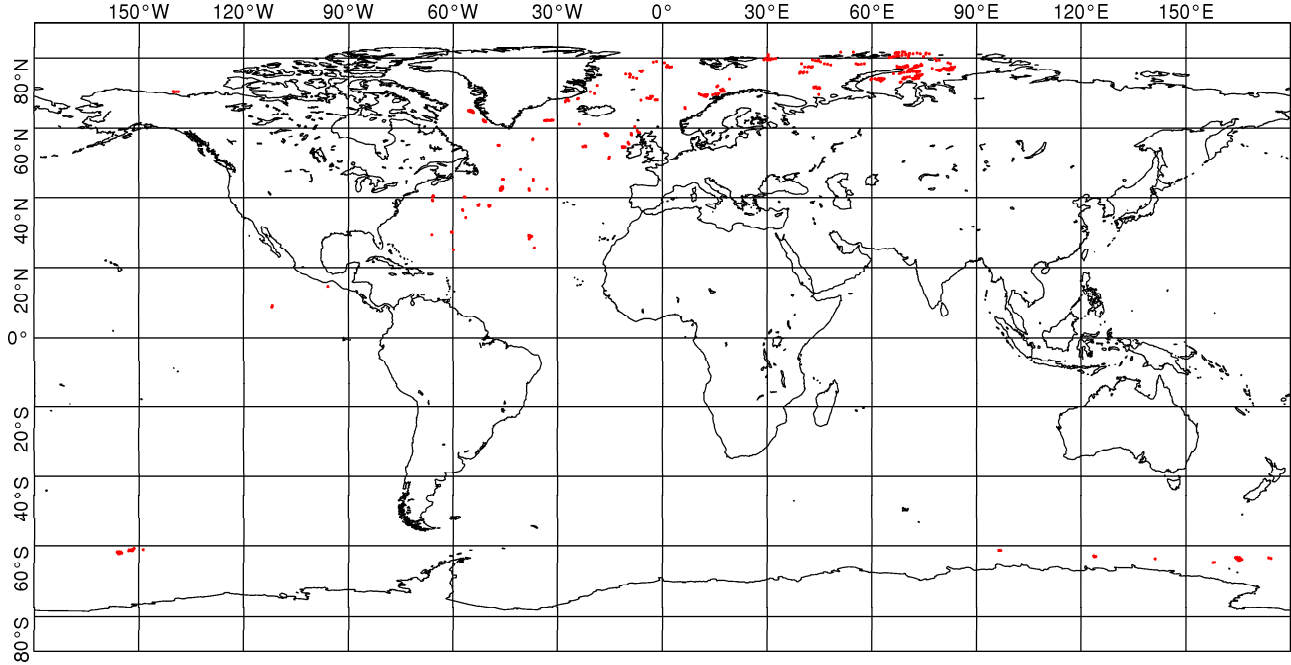


Figure 10

CYCLE 162, 2010101900 to 2010112218, QC on ESA flags



UWI winds more than 8 m/s stronger than ECMWF First Guess  
CYCLE 162, 2010101900 to 2010112218, QC on ESA flags

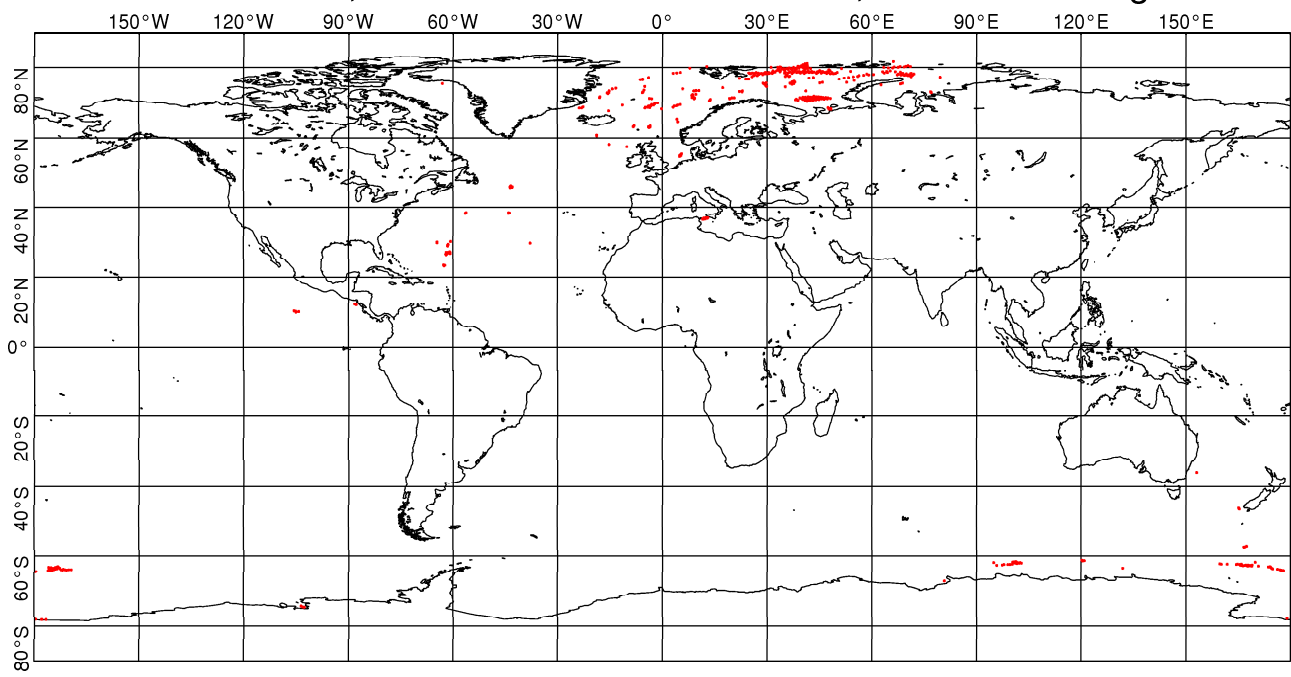
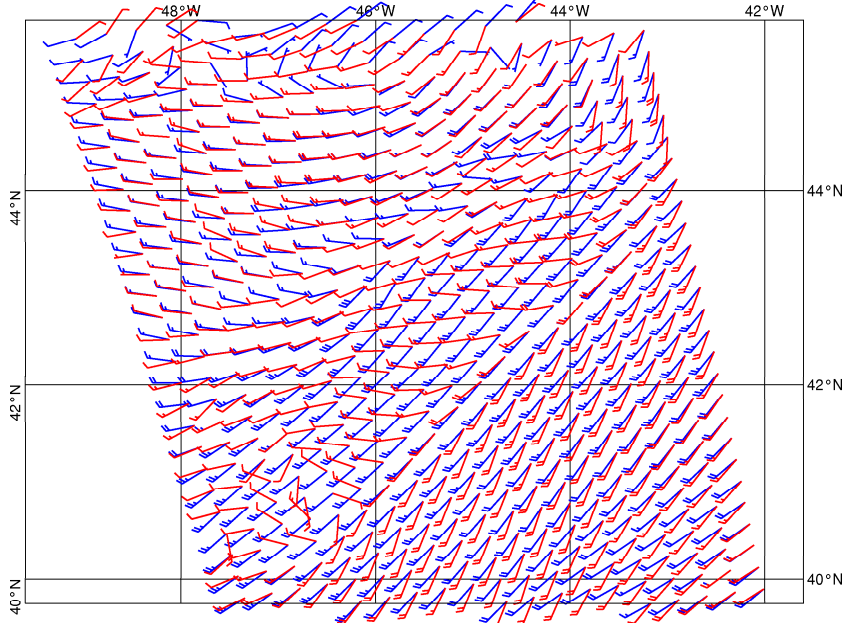


Figure 11



UWI winds (red) versus ECMWF FG winds (blue)  
North Atlantic 20101102 01:22 UTC



UWI winds (red) versus ECMWF FG winds (blue)  
Mediterranean 20101108 21:40 UTC

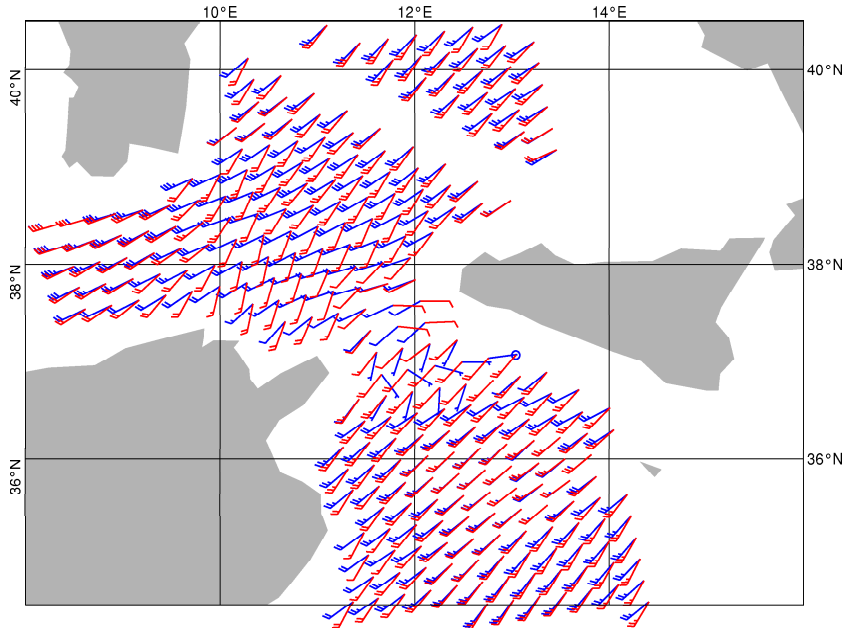


Figure 12

ECMWF 3-hourly First-Guess winds versus UWI winds  
from 2010101900 to 2010112218  
= 747257, db contour levels, 5 db step, 1st level at 3.7 db  
 $m(y-x) = -0.89$   $sd(y-x) = 1.52$   $sdx = 3.86$   $sd_y = 3.59$   $pcxy = 0.958$

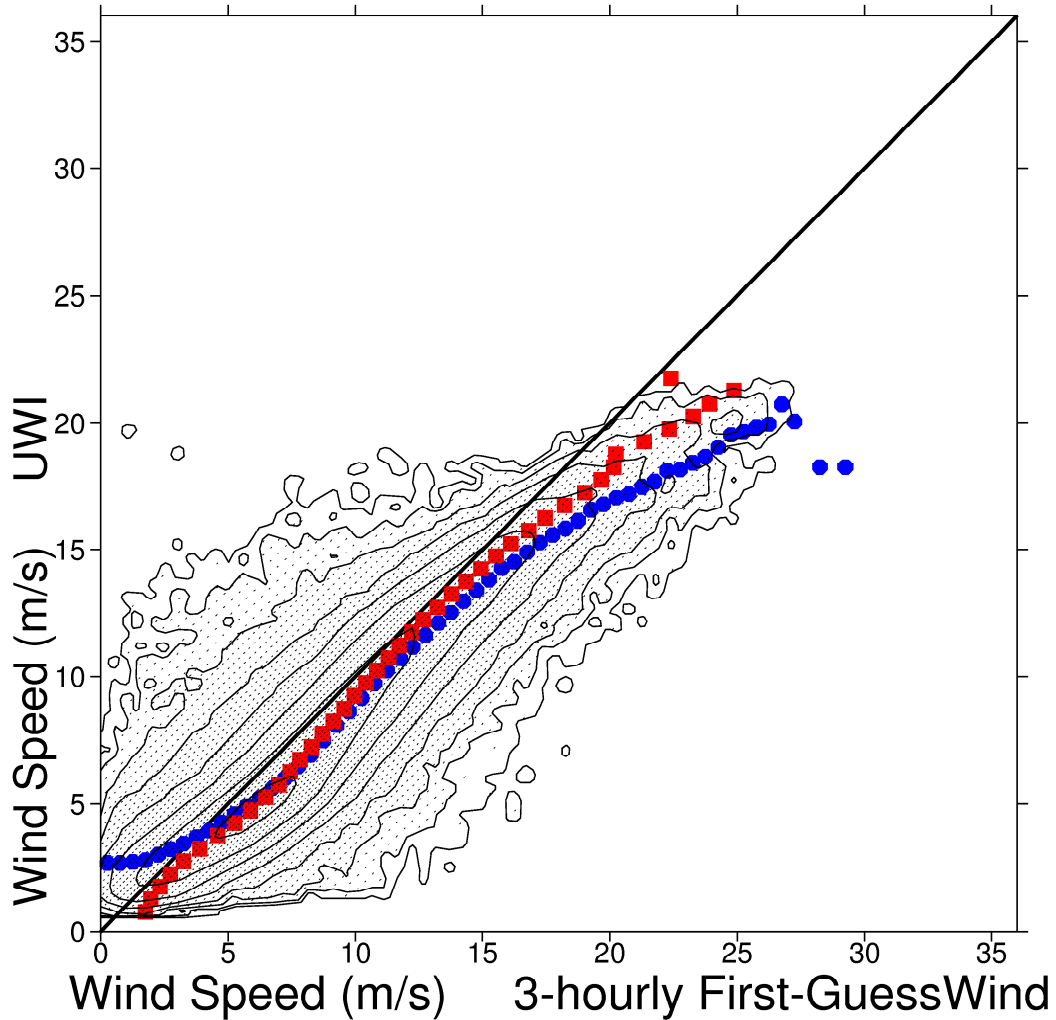


Figure 13

ECMWF 3-hourly First-Guess winds versus UWI winds  
from 2010101900 to 2010112218

= 621984 ( |f| gt 4.00 m/s ), db contour levels, 5 db step, 1st level at 2.9 db  
m(y-x)= -3.01 sd(y-x)= 31.57 sdx=113.08 sdy=113.26 pcxy= 0.980

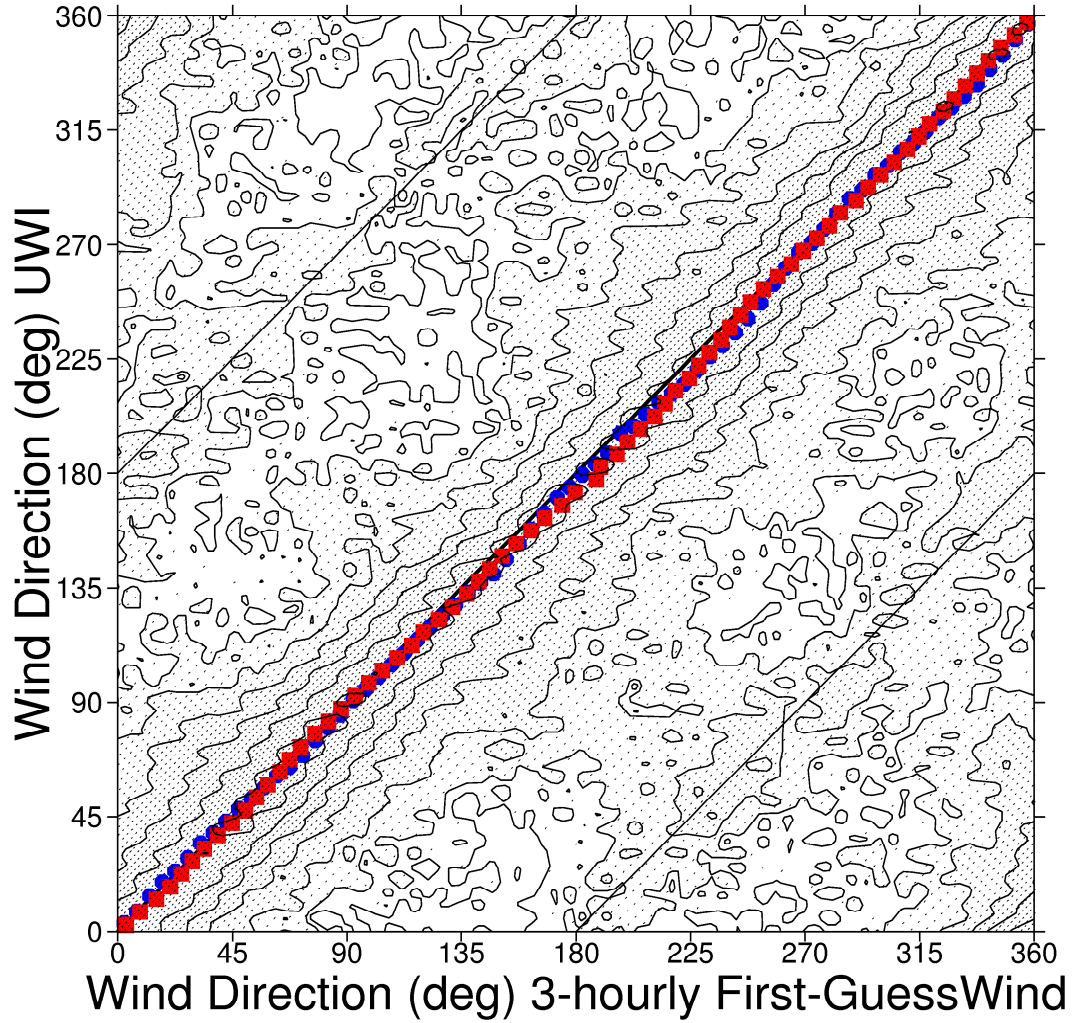


Figure 14

ECMWF 3-hourly First-Guess winds versus CMOD4 winds  
from 2010101900 to 2010112218

= 741504, db contour levels, 5 db step, 1st level at 3.7 db  
 $m(y-x) = -0.87$   $sd(y-x) = 1.52$   $sdx = 3.83$   $sd_y = 3.58$   $pcxy = 0.958$

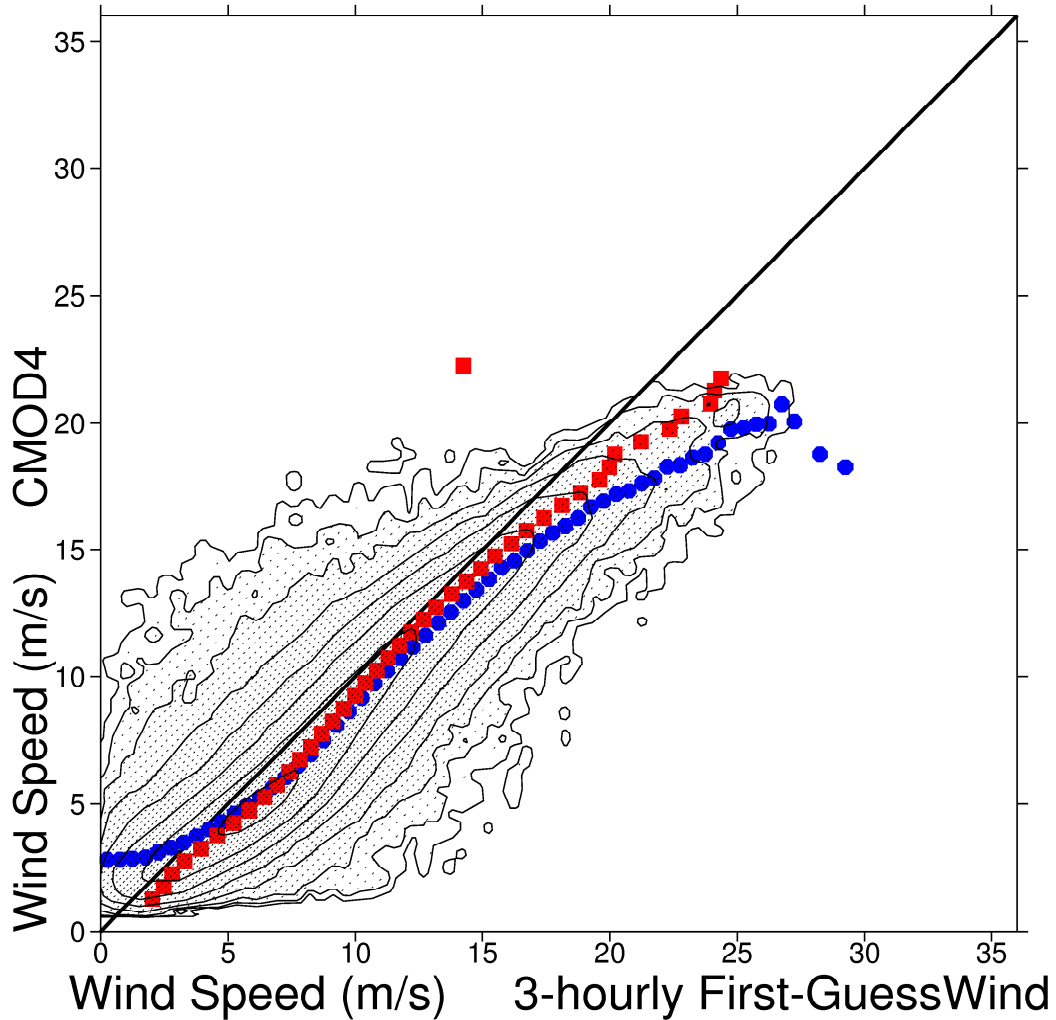


Figure 15

ECMWF 3-hourly First-Guess winds versus CMOD5 winds  
from 2010101900 to 2010112218

= 732198, db contour levels, 5 db step, 1st level at 3.6 db  
 $m(y-x) = -0.35$   $sd(y-x) = 1.46$   $sdx = 3.80$   $sd_y = 3.67$   $pcxy = 0.961$

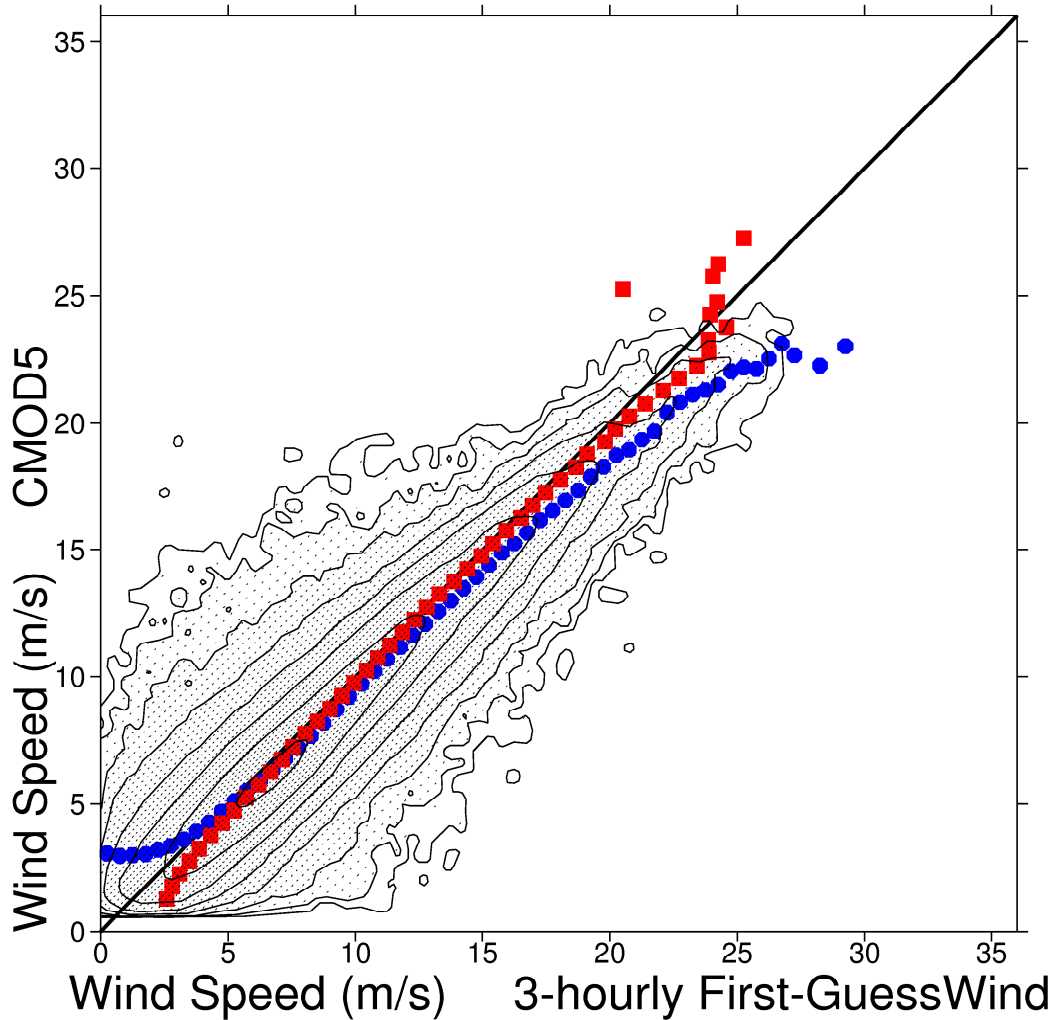


Figure 16